34th Annual International Conference of the IEEE EMBS
San Diego, California USA, 28 August - 1 September, 2012

Axon terminal polarization induced by weak uniform DC electric fields: a modeling study

Mattia Arlotti, Asif Rahman, Preet Minhas, and Marom Bikson, *Member, IEEE*

Abstract— **Uniform steady state (DC) electric fields, like those generated during transcranial direct current stimulation (tDCS), can affect neuronal excitability depending on field direction and neuronal morphology. In addition to somatic polarization, subthreshold membrane polarization of axon compartments can play a significant role in modulating synaptic efficacy. The aim of this study is to provide an estimation of axon terminal polarization in a weak uniform subthreshold electric field. Simulations based on 3D morphology reconstructions and simplified models indicate that for axons having long final branches compared to the local space constant (L>4λ) the terminal polarization converges to Eλ for electric fields oriented in the same direction as the branch. In particular we determined how and when analytical approximations could be extended to real cases when considering maximal potential polarization during weak DC stimulation.**

I. Introduction

Transcranial direct current stimulation (tDCS) is a non-invasive brain stimulation method to modulate neuronal excitability using direct currents injected via scalp electrodes. tDCS generates weak electric fields, that are uniform on the scale of single neurons/cortical columns ("quasi-uniform"), with both radial (normal to the cortical surface) and tangential (parallel to the cortical surface) components. For low amplitude currents (<1 mA) weak DC electric fields can modulate neuronal excitability by membrane potential polarization. Therapeutic applications are designed to increase or decrease cortical excitability based only on the induced somatic polarization of cortical pyramidal neurons. However, *in vitro* experiments suggested that, in addition to somatic polarization, the axonal and dendritic compartments also play a role in determining the neuronal modulation by DC stimulation, especially when considering processing of synaptic inputs [1, 2]. Quantifying the state of polarization of axon terminations induced by weak DC electric fields can help explain mechanisms of tDCS and thus enable rational protocol design.

Experimental characterization of axonal polarization in animal models is complex and generally indirect due to structure and small dimensions of final axonal branches. Though interestingly, polarization of the soma can modify action potentials at the axonal termination and affect excitatory post-synaptic potential amplitudes [3-5].

There are established analytical models to predict polarization of a semi-infinite or finite straight axon under external electric fields [6-9]; in particular for uniform electric fields the maximum polarization occurs at the terminals [9]. However, the real geometry of axons is evidently more complex and the details of morphology will affect polarization. For example, in the case of branches and incremental bends, semi-infinite approximations may not be valid. Even when numerical simulations are implemented, much of the (distal) axonal arborization is absent and it is not clear what quantitative inferences can be made for thalamocortical and corticocortical projections. Therefore, it is unclear what the magnitude of axon terminal polarization is in realistic cortical afferents during weak DC stimulation, such as tDCS with radial and tangential directed currents.

In this study we integrated information from numerical and analytical solutions of 3D reconstructed neurons and simplified cable models, respectively, in order to infer a general rule to explain (maximum) axon terminal steady state polarization under a uniform electric field. While the diversity of neuronal morphology and biophysics indicates individual neuron models may be required, a heuristic "rule of thumb" is desired for *maximum* cortical DC stimulation of axons. In addition, we consider polarization may be dependent or independent of somatic polarization.

TABLE I

Nomenclature		
Variables	***Definition***	***Unit***
Vm	Membrane potential	mV
Ve	Extracellular potential	mV
τ	Time constant	s
λ	Space constant	mm
s	Local coordinate of the fiber	mm
t	Time	s
E	External electric field	mV/mm

II. Methods

A. Cable Theory Formulation

Starting from the cable theory [6], it is possible to formalize the effect of extracellular stimulation for a uniform fiber in the continuous equation [7]:

$$\frac{\partial V_m}{\partial t} + \lambda^2 \frac{\partial^2 V_m}{\partial s^2} - V_m = \lambda^2 \frac{\partial^2 V_e}{\partial s^2} \qquad (1)$$

Research supported by the National Institutes of Health and the Wallace H. Coulter Foundation.

A. Rahman, P. Minhas and M. Bikson are with the Biomedical Engineering Department, City College of The City University of New York, NY, 10031 USA (contact: 212-650-6791; fax: 212-6506727; e-mail: bikson@ ccny.cuny.edu).

M. Arlotti is with the Department of Electronics, Computer Science and Systems, University of Bologna, Cesena, Italy.

For uniform electric fields applied to a finite straight fiber the activating function (right side of (1)) is zero along the membrane except at the ends. In this case a simple analytical solution exists relating terminal polarization with the space constant and the length of the fiber. Considering the electric field in the same direction of the fiber, for $l < \lambda$ (where l is the physical length of the cable) the values of the terminal polarization in steady state conditions are ±EL/2 instead for $l > 4\lambda$ the terminal polarizations are ±Eλ. This is valid for sealed-end boundary conditions, relaxing that constraint changes the terminal polarization [8]. The effect of the electric field on the membrane potential is strictly related to its projection along the fiber:

$$\lambda^2 \frac{\partial^2 V_e}{\partial s^2} = \lambda^2 \frac{\partial^2 (\vec{E} \cdot \hat{s})}{\partial s^2} \tag{2}$$

For neurons (axons) with increased morphological and biophysical details (compartment diameter, membrane conductance), the polarization solution quickly increases the problem complexity [9] as it is necessary to consider the polarization of each compartment and then the axial currents; such that for "realistic" cases we have no analytical solutions. However, with the goal of understanding when approximations of polarization are valid (see Results), we derived the analytical solution for a cable with a bend (Fig. 1) and seal-end boundary conditions:

$$\frac{\partial V_i}{\partial s} = 0 \qquad s = 0 \vee s = l \tag{3}$$

where $l = l_0 + l_1$ (l_0 and l_1 are the physical length of the two segments, mm) because:

$$\frac{\partial V_m}{\partial s} = \frac{\partial V_i}{\partial s} - \frac{\partial V_e}{\partial s} \tag{4}$$

$$\frac{\partial V_m}{\partial s} = E \qquad s = 0 \tag{5}$$

$$\frac{\partial V_m}{\partial s} = E\cos(\theta) \qquad s = l\,. \tag{6}$$

Under these assumptions the terminal polarization (V_t) varies as (Fig. 1):

$$V_t = \frac{E\lambda_1 \cos(\theta)(\cosh(L) - \cosh(L_0))}{\sinh(L)} + \frac{E\lambda_0(\cosh(L_0) - 1)}{\sinh(L)} \tag{7}$$

where $L = l_0/\lambda_0 + l_1/\lambda_1$, $L_0 = l_0/\lambda_0$ and $L_1 = l_1/\lambda_1$.

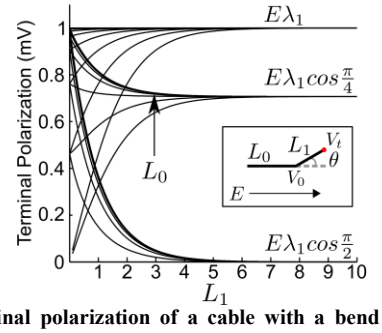

Figure 1. **Terminal polarization of a cable with a bend in a uniform electric field along the direction of the first segment, uniform distribution of internal passive parameters and constant diameter**. The terminal polarization varies as function of L_1, L_0 and θ. For L_1>4 the terminal polarization always converges to $E\lambda_1\cos(\theta)$ irrespective of the value of L_0. For $L_1 < 4$ the terminal polarization increases with L_0. $E\lambda_1$ is the maximal value for the given configuration.

B. Neuron Modeling

Cortical neuron polarization, specifically of axonal terminations, in uniform electric fields were implemented a computational model in NEURON. The 3D neuron morphologies were taken from the Neuromorpho database (www.neuromorpho.org), in particular 8 different models of pyramidal cell (LII\III, LIV, LV) of rat somatosensory cortex were chosen (ID: NMO_0116, NMO_00348, NMO_00410, NMO_00417, NMO_01134, NMO_01132, NMO_01135, NMO_01112). In all cases, 1 V/m uniform electric fields were applied through the built-in function *e_extracellular(x)*, assuming the conductivity of the medium was constant over the extracellular space.

The following passive properties were added to each neuron uniformly: an internal resistance, Ri, of 155 kΩcm, a membrane resistance, Rm, of 70 kΩcm², [10], and the default membrane capacitance, Cm, of 1 μF/cm.

C. Mirror Estimate

The Mirror Estimate has shown to be a good predictor of the steady state membrane polarization under the effect of external electric fields for *compact* structures [11]. For real neuron morphologies the value of the membrane potential for each compartment (k) is given by:

$$V_m^k = -V_e^k + \frac{\sum_{j=0}^{N} \frac{V_e^j}{(\lambda^j)^2}}{\sum_{j=0}^{N} \frac{1}{(\lambda^j)^2}} \tag{8}$$

where N is the total number of compartments.

In order to quantify the goodness of the estimation we used the following matching criteria [5]:

$$C_{mirror} = \langle V_m, mirror \rangle / \sqrt{\langle V_m, V_m \rangle \times \langle mirror, mirror \rangle} \tag{9}$$

III. RESULTS

A. Axon terminal polarization

Solving the numerical models for radial and tangential fields (Fig. 3, B1-2) reveals that the effects of uniform electric fields on axonal terminations is influenced by numerous factors including the direction of the electric field and the orientation and the length of the last branch (Fig. 3, C1-2). By incrementally rotating the electric field on the "xy" plane (Fig. 3, B3), we found the optimal orientation (the direction that produces maximum terminal polarization in the specific branch) for each final branch. Importantly, we show that for increasing lengths in the optimal direction the axonal terminal polarization approaches Eλ (Fig. 3, C3) (the space constant is calculated with the diameter of the final branch and then normalized in order to compare the results), and the optimal direction becomes the final branch direction.

B. Axon terminal polarization: Analytical approximations

Noting that maximal polarization in a realistic neuron model approaches that predicted for a simple semi-infinite axon, we next consider when/how heuristic approximations can be used to predict terminal polarization.

For a fiber with a single (final) bend, based on (7), in the case of uniformly distributed passive parameters and constant diameter, Eλ is the maximum polarization of the

terminal (Fig. 1). In real geometries, the axon diameter remains constant after 3 branching points [5] and the internal parameter distribution can be considered uniform. Eλ is the maximum value of the terminal polarization irrespective of the length of the final branch (Fig. 3A). So when is maximum polarization achieved and how well does the final-bend approximations explain the numerical results?

In order to formalize the problem we modeled the last branch as a straight finite fiber. The solution for the terminal polarization depends on the boundary condition at the terminal (s_t) and the boundary condition at the last branch point. At the terminal boundary condition is:

$$\frac{\partial V_m}{\partial s} = E\cos(\theta) \qquad s = s_t \qquad (10)$$

The branch boundary is however dependent on morphology of the entire neuron and cannot be solved analytically. Therefore, we can compute this boundary condition, the polarization at the branch point, numerically and then use this value in the hybrid numerical/analytical solution. Alternatively this value can be clamped to fixed arbitrary value, such as 0. In either case, given the last branch point polarization value V_0 and fixing the length equal to l (the length of the last branch) we obtain (11) where L = 1/λ.

$$V_t = E\lambda\cos(\theta)\tanh(L) + V_0/\cosh(L) \qquad (11)$$

This expression is a static formalization of the problem of the last branch (Fig. 3, A), because V_0 changes with L. It is useful to collapse the 3D problem into a 1D cable problem for the last branch. The shrinking in the z-direction due to the slice procedures results in $l_{xy} = l$.

In fact, using the values of V_0 and L taken from the numerical solution, the expression matches the results of the 3D computational model (Fig. 3, D1-3, green points).

Note by assuming the value V_0 = 0, tanh(L) = 1, the terminal polarization is:

$$V_t = E\lambda\cos(\theta) \qquad (12)$$

which is equivalent to considering a semi-infinite axon.

The error per 1 V/m between (11, 12) and the numerical solution is comparable for electrotonic length >2 (Fig. 3, D1-3), on the contrary for smaller lengths the error increases using (12) and remains close to zero for (11). Without numerical solutions we cannot know the optimal orientation and we assume θ=0 for (12).

C. *Axon terminal polarization: Mirror Estimate*

As expected, polarization of terminations electrotonically uncoupled with the final branch point is not accurately predicted by the Mirror Estimate (Fig. 3, D1-3, purple points). We extended the analysis to neurons with axonal arborizations for two different set of passive membrane parameters (Ri=155 Ωcm, Rm=70 KΩcm² and Ri=155 Ωcm, Rm=17.5 KΩcm²). We also considered accuracy with only the dendrite reconstruction (by removing the axon) and the complete neuron. Finally, we compared the mirror estimate and the output of the NEURON model (Fig. 2) and we used (9) to evaluate the estimation. Considering *only* the dendritic reconstruction the estimation is accurate for both sets of membrane parameters, but for the complete neuron, with intact axon, the matching criteria (9) decreases from 0.92 to

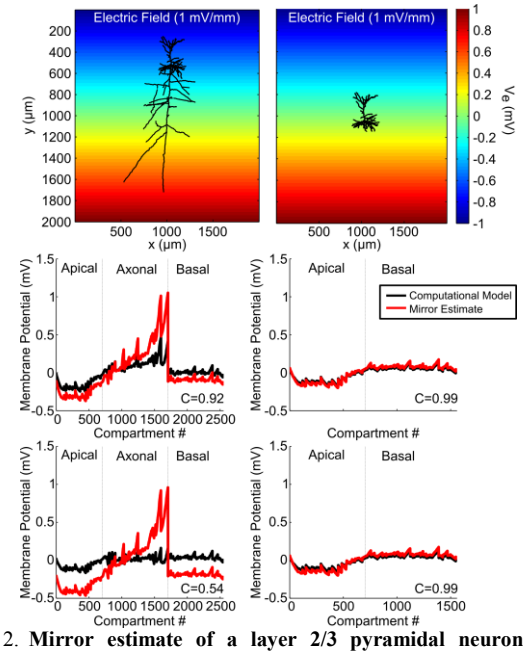

Figure 2. **Mirror estimate of a layer 2/3 pyramidal neuron of rat somatosensory cortex.** On the top: Extracellular potential distribution for 1V/m along the neuron with axon (left) and without (right). On the middle: mirror estimate (red) and computational model of extracellular (black) comparison for Ri=155Ωcm, Rm=70 KΩcm². On the bottom: mirror estimate (red) and computational model of extracellular (black) comparison for Ri=155Ωcm, Rm=17.5 KΩcm². The maximum error occurs at the axonal compartments for the smaller of the space constant, geometrical features and passive parameters affect the mirror estimate.

0.54. The maximum absolute error for the first set of parameters occurs at axonal compartments with a peak of 0.63 mV. In fact the matching criteria proposed in (9) gives an estimation of the correlation between two curves (e.g. for two sinusoidal function with different amplitude but equal phase C=1). The closeness of the mirror estimate to the numerically predicted membrane potential decreases with the loss of electrotonic compactness of the axonal arborization (Fig. 2).

IV. Discussion

Numerical simulations of cortical neuron polarization indicated that terminal polarization is a complex function of neuronal morphology relative to the applied electric field, with no initially apparent relationship between terminal branch length or angle relative to the field, and terminal-coupling constant. However, for individual branches, consideration of the polarization at the optimal electric field angle reveals an asymptotic approach to Eλ for branch lengths greater than 4λ. Similarly, the analytical approximation for a semi-infinite axon (Eλcosθ) was accurate for branch lengths >4λ; deviations for shorter branches were fully accounted for by considering membrane polarization at the respective branch. As expected, the mirror estimate, which assumes compact structures, was not accurate for axon terminals.

The proposed model has two noted limitations: complete axonal reconstruction and parameterization. Unfortunately entire reconstructions of axonal arborization from slice preparation are limited by cutting operation and visualization

problems [3, 12]. Most of the computational models try to avoid the issue by adding artificial axons to real dendritic trees [3, 13, 14]. The proposed model assumes uniform distribution of passive parameters, but because we are interested in axon terminals the results can easily be extended whatever the local values of the space constant are. Also not included are active membrane proprieties, which may also be relevant in the spread of subthreshold potentials [4]. In the present analysis we chose all pyramidal neurons because they are, with a few exceptions, the only projection neuron of the cerebral cortex [12], but the analysis is valid also for other classes of neurons. The model limitations (axonal reconstruction and parameterization) can be solved with the availability of experimental data, which can confirm when our heuristic prediction is correct and when the results can be extended to humans cells. Finally, we applied the quasi-uniform assumption, but changes in electric field along extended axons may be relevant [15, 16].

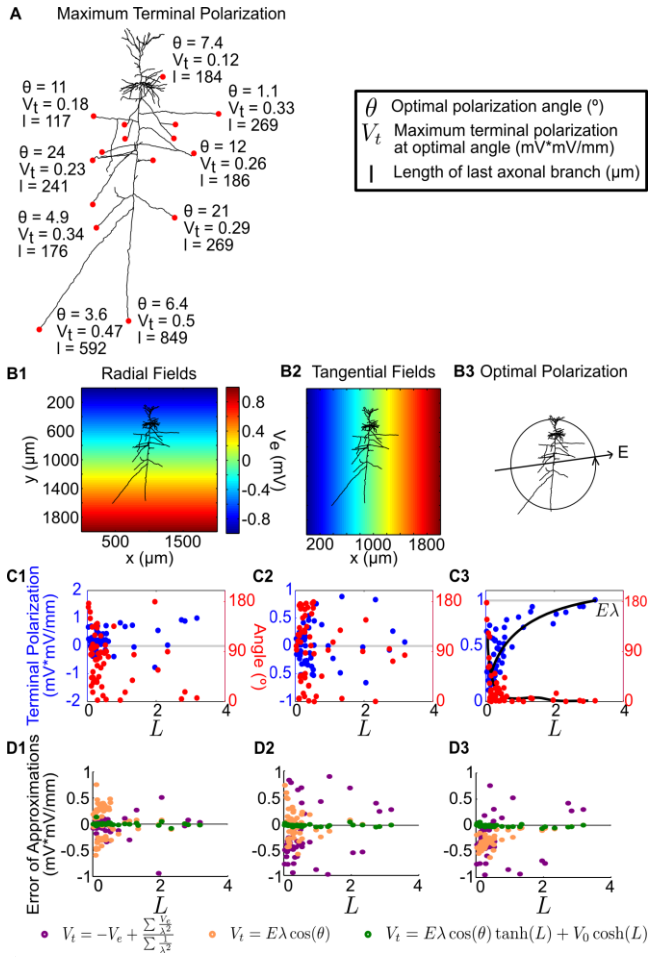

Figure 3. **Terminal polarization by uniform DC electric fields using neuron compartment model and analytical/hybrid approximations.** ***A***, Maximum terminal polarization (V_t) and corresponding optimal polarization angle (θ) between the last axonal branch and the electric field direction at length (*l*) of the terminal from the last bend. ***B1-2***, Distribution of extracellular potential for radial and tangential uniform electric fields. ***B3***, The field is oriented in the direction that maximizes the terminal polarization. ***C1***, For radial electric fields, numerically calculated terminal polarization is plotted for the electrotonic length of the last axon branch (blue), the angle of the last branch relative to the field is also shown (red). ***C2***, For tangential electric fields, numerically calculated terminal polarization is plotted for the electrotonic length of the last axon branch (blue), the angle of the last branch relative to the field is also shown (red). ***C3***, Numerically determined maximal terminal polarization (blue) for an optimally oriented electric field (angle blue) plotted for the electrotonic length of the axon branch is evaluated. Maximum terminal polarization approached Eλ (with a field parallel to the last branch) as length, *l*, approached 4λ. ***D1***, Error of the approximation for E = 1 V/m in radial direction. ***D2***, Error of the approximation for E = 1 V/m in tangential direction. ***D3***, Error of the approximation for E = 1 V/m in optimal direction. The best approximation (green dots) of terminal polarization (V_t) considers the hybrid solution where the terminal polarization is weighted and coupled with the polarization of the bend point (V_o). The semi-infinite approximation is valid for long final segments ($l > 4\lambda$) with deviation from the numerical solution fully accounted for by the branch point voltage (V_o, hybrid model).

REFERENCES

[1] Bikson M, Inoue M, Akiyama H, Deans JK, Fox JE, Miyakawa H, Jefferys JG. "Effect of uniform extracellular DC electric fields on excitability in rat hippocampal slices in vitro" J Physiol. 2004; 557(Pt 1):175-90.

[2] Radman T, Ramos RL, Brumberg JC, Bikson M. "Role of cortical cell type and morphology in subthreshold and suprathreshold uniform electric field stimulation in vitro" Brain stimul. 2009; 2(4):215-28.

[3] Shu Y, Hasenstaub A, Duque A, Yu Y, McCormick DA. "Modulation of intracortical synaptic potentials by presynaptic somatic membrane potential" Nature. 2006;441(7094):761-5.

[4] Foust AJ, Yu Y, Popovic M, Zecevic D, McCormick DA. "Somatic membrane potential and Kv1 channels control spike repolarization in cortical axon collaterals and presynaptic boutons" J Neurosci. 2011;31(43):15490-8.

[5] Sasaki T, Matsuki N, Ikegaya Y. "Effect of axonal topology on the somatic modulation of synaptic output" J Neurosci. 2012;32(8):2868-76.

[6] McNeal DR. "Analysis of a Model for Excitation of Myelinated Nerve" IEEE Trans Biomed Eng. 1976;23(4):329-37.

[7] Rattay F. "Analysis of Models for External Stimulation of Axons" IEEE Trans Biomed Eng. 1986;33(10):974-7.

[8] Rubinstein JT. "Axon terminal conditions for electrical stimulation" IEEE Trans Biomed Eng. 1993;40(7):654-63.

[9] Tranchina D, Nicholson C. "A model for the depolarization of neurons by extrinsically applied electric fields" Biophys J. 1986;50(6):1139-56.

[10] Markram H, Wang Y, Tsodyks M. "Differential signaling via the same axon of neocortical pyramidal neurons" Proc Natl Acad Sci U S A. 1998;95(9):5323-8.

[11] Joucla S, Yvert B. "The mirror estimate: an intuitive predictor of membrane polarization during extracellular stimulation." Biophys J. 2009;96(9):3495-508.

[12] Romand S, Wang Y, Toledo-Rodriguez M, Markram H. "Morphological development of thick-tufted layer V pyramidal cells in the rat somatosensory cortex", Front Neuroanat. 2011;5:5.

[13] Mainen ZF & Sejnowski TJ, "Influence of dendritic pattern in model neocortical neurons", Nature. 1996;382(6589):363-6.

[14] Pashut T, Wolfus S, Friedman A, Lavidor M, Bar-Gad I, Yeshurun Y, Korngreen A. "Mechanisms of magnetic stimulation of central nervous system neurons", PLoS Comput Biol. 2011;7(3):e1002022

[15] Miranda PC, Correia L, Salvador R, Basser PJ. "The Role of Tissue Heterogeneity in Neural Stimulation by Applied Electric Fields" Conf Proc IEEE Eng Med Biol Soc. 2007;2007:1715-8.

[16] Miranda PC, Correia L, Salvador R, Basser PJ. "Tissue heterogeneity as a mechanism for localized neural stimulation by applied electric fields." Phys Med Biol. 2007 Sep 21;52(18):5603-17.